

High-Resolution Climate Projections Using Diffusion-Based Downscaling of a Lightweight Climate Emulator

Haiwen Guan¹, Moein Darman², Dibyajyoti Chakraborty¹, Troy Arcomano³,
Ashesh Chattopadhyay², Romit Maulik⁴

¹Information Sciences and Technology, The Pennsylvania State University, University Park, Pennsylvania

²Department of Applied Mathematics, University of California, Santa Cruz, California

³Allen Institute for Artificial Intelligence (AI2), Seattle, Washington

⁴School of Mechanical Engineering, Purdue University, West Lafayette, Indiana

Key Points:

- We introduce a deep learning framework to downscale a coarse-grid climate emulator output from 300 km to 25 km resolution.
- Data-driven super-resolution models can recover fine-resolution climatological statistics using inputs from a coarse-grained emulator.
- The framework proposes an alternative to directly training climate emulators at high resolution.

Abstract

The proliferation of data-driven models in weather and climate sciences has marked a significant paradigm shift, with advanced models demonstrating exceptional skill in medium-range forecasting. However, these models are often limited by long-term instabilities, climatological drift, and substantial computational costs during training and inference, restricting their broader application for climate studies. Addressing these limitations, Guan et al. (2024) introduced LUCIE, a lightweight, physically consistent climate emulator utilizing a Spherical Fourier Neural Operator (SFNO) architecture. This model is able to reproduce accurate long-term statistics including climatological mean and seasonal variability. However, LUCIE's native resolution (300 km) is inadequate for detailed regional impact assessments. To overcome this limitation, we introduce a deep learning-based downscaling framework, leveraging probabilistic diffusion-based generative models with conditional and posterior sampling frameworks. These models downscale coarse LUCIE outputs to 25 km resolution. They are trained on approximately 14,000 ERA5 timesteps spanning 2000–2009 and evaluated on LUCIE predictions from 2010 to 2020. Model performance is assessed through diverse metrics, including latitude-averaged RMSE, power spectrum, probability density functions and First Empirical Orthogonal Function of the zonal wind. We observe that the proposed approach is able to preserve the coarse-grained dynamics from LUCIE while generating fine-scaled climatological statistics at ≈ 28 km resolution.

Plain Language Summary

Advanced computer models are increasingly used to predict weather and climate. While powerful, these models often face challenges such as becoming unstable over long periods or being too expensive to run at high detail. Researchers recently developed LUCIE, a data-driven climate model that accurately and computationally efficiently predicts climate trends for over 1000 years. However, LUCIE provides forecasts at low resolution, which are not detailed enough for local climate assessments needed by communities and policymakers. In our study, we adopt a data-driven super-resolution framework to transform LUCIE's low-resolution predictions into high-resolution fields. We use advanced artificial intelligence techniques that take coarse climate data and produce high-resolution outputs suitable for regional climate studies. We test our models rigorously using real-world data and compared their performance using various quality measures. Our results show that this method accurately preserves large-scale climate features while providing detailed local information, offering a pathway to detailed climate planning and adaptation efforts.

1 Introduction

Access to high-resolution climate and weather data is critical for assessing regional risks, from hydrological modeling and energy forecasting to urban heat-stress planning. Key impact phenomena, such as localized convective precipitation and heatwaves, are governed by fine-scale features like topography and land cover that coarse global climate products fundamentally cannot resolve (Schwingshackl et al., 2024).

Generating these fine-scale datasets over large domains or long (decadal to centennial) periods presents a major computational bottleneck. While dynamical downscaling via regional climate models (RCMs) provides the necessary physical detail, its computational expense is prohibitive, severely limiting ensemble sizes and simulation lengths (Skamarock et al., 2019; Giorgi, 2019). Observational and reanalysis products, conversely, often lack the required spatial resolution, particularly in data-sparse regions.

Statistical and machine learning (ML) downscaling methods have emerged as a computationally efficient alternative (Maraun & Widmann, 2018; Rampal et al., 2024; Sachin-

dra et al., 2018). This field has rapidly evolved from classical statistical mappings to deep learning architectures, including convolutional networks (CNNs) (Vandal et al., 2017; Baño-Medina et al., 2020), Generative Adversarial Networks (GANs) (Zhu et al., 2020; Wang et al., 2023), and neural operators (Wei & Zhang, 2023; Jiang et al., 2023). More recently, generative diffusion models have shown exceptional promise, demonstrating an ability to produce high-fidelity, stochastic reconstructions of climate fields (Tu, Xu, et al., 2025; Tu, Fei, et al., 2025).

Despite their success, many ML downscaling algorithms face critical limitations. Performance can degrade significantly under distributional shifts, such as when applied to geographic regions not seen during training (Harder et al., 2025). Furthermore, a crucial and often overlooked challenge arises when models trained on “perfect” coarsened reanalysis data are applied to inputs from an independent climate model or emulator. As recent work highlights, this “imperfect input” setting often leads to degraded spatial consistency and an underestimation of extremes (Reddy et al., 2025).

This challenge is particularly relevant given the concurrent rise of deep learning-based climate emulators. Models like LUCIE offer long-term, stable, and physically-consistent simulations at a fraction of the cost of traditional GCMs (Guan et al., 2025). However, their utility for impact assessment is limited by their coarse native spatial resolution (e.g., 300 km), which is precisely the problem downscaling aims to solve.

In this paper, we propose and evaluate a novel framework that directly bridges the gap between efficient climate emulation and high-resolution impact assessment by coupling a coarse-grained emulator (LUCIE) with a suite of data-driven super-resolution (SR) models. Throughout this study, we use the terms downscaling and super-resolution interchangeably. We contrast deterministic architectures—specifically a Spherical Fourier Neural Operator (SFNO-SR)—against modern probabilistic diffusion models, including a Conditional EDM framework and a Posterior Sampling approach. The SR models are trained on ERA5 reanalysis data (2000–2009) and subsequently evaluated on their ability to super-resolve outputs from the LUCIE emulator for a distinct period (2010–2018). Due to the chaotic nature of climate dynamics and unavoidable spectral biases, machine learning climate emulations are inherently imperfect. This setup allows us to test the models’ robustness in an “imperfect input” setting, where the SR task is to resolve fine-scale details implied by the emulator’s coarse state rather than clean reanalysis. We argue that the inherent discrepancies between reanalysis data and emulator inference necessitate the use of generative modeling. Unlike deterministic baselines that produce a single averaged solution—often resulting in spatial blurring—probabilistic frameworks treat the emulator’s imperfections as a source of conditional uncertainty.

The development of machine learning for atmospheric downscaling has progressed from early CNN-based methods (Nguyen et al., 2022; Vandal et al., 2017) to Generative Adversarial Networks (GANs), which first demonstrated the ability to recover high-frequency power spectra in wind and solar data (Stengel et al., 2020). More recently, the field has seen a surge in generative diffusion frameworks that set new benchmarks for physical realism. Watt and Mansfield (Mardani et al., 2025) established the effectiveness of the EDM diffusion framework for climate variables, demonstrating its superior accuracy and spectral fidelity over deterministic baselines in idealized settings. Similarly, CorrDiff (Mardani et al., 2025) utilizes a multi-step diffusion framework to bridge the gap between global weather predictions and km-scale observations. However, while CorrDiff excels at capturing fine-scale turbulent structures, its application remains primarily localized or patch-based, lacking a framework for continuous global SR. Furthermore, while modern architectures like the Super-Resolution Neural Operator (SRNO) (Wei & Zhang, 2023) offer resolution-invariant solvers, they are often designed as general-purpose tools rather than specialized frameworks for global climate constraints. Recent work by Lopez et al. (Lopez-Gomez et al., 2025) has advocated for a modular “two-stage” dynamical-generative approach to downscale climate ensembles, reflecting a shift toward decoupled modeling

frameworks. However, while their work utilizes intermediate dynamical models to target specific regional domains, our framework implements a fully data-driven, global pipeline. By coupling the LUCIE emulator directly with super-resolution models, we provide a computationally efficient alternative that maintains statistical and dynamical consistency across the entire globe.

We evaluate the framework using a comprehensive suite of diagnostics designed to measure both point-wise accuracy and global physical consistency. In addition to standard spatial metrics, we employ zonal averaged climatology and spectral analysis to assess the models' ability to reconstruct the high-wavenumber variance and “roughness” of atmospheric turbulence. Furthermore, we use Empirical Orthogonal Function (EOF) analysis to verify that the SR process preserves the primary modes of climate variability, such as the annular structures of the zonal wind.

It is worth highlighting that atmospheric SR is fundamentally an ill-posed, “one-to-many” problem, where a single coarse input can physically correspond to multiple high-resolution realizations. While deterministic models like SFNO-SR can capture large-scale patterns, they provide only a single estimate. In contrast, the probabilistic nature of diffusion models aligns more naturally with the inherent uncertainty of the downscaling task by generating ensembles of plausible states. By recovering missing fine-scale details such as orographic precipitation and sharp thermal gradients, this coupled framework allows lightweight emulators like LUCIE to be used for fine-scale studies—such as monsoon tracking or wildfire risk assessment—that were previously impossible at coarse resolutions.

The remainder of this paper is organized as follows: Section 2 describes data sources for training and validation of our downscaling algorithm, specifics of our deep learning architectures, and subsequent evaluation strategies for the trained models. Section 3 presents the experimental results, including seasonal climatology and spectral fidelity. Section 4 discusses the broader implications of these findings for climate modeling and offers concluding remarks and future perspectives.

2 Data and Methods

The primary goal of this effort is to generate high-fidelity, physically consistent climate data at a target resolution of approximately 25 km (720×1440), given predictions from a coarse-grained emulator at a resolution of approximately 300 km (48×96). To accomplish this, we construct a coupling scenario as shown in Figure 1. A coarse-grained atmospheric forecast is initialized using LUCIE on a T30 Gridded ERA5 state at a timestep of 6 hours. Subsequently, the downscaling model is applied as a postprocessing step at each timestep of the prediction. The fine scale state is *not* reused to initialize the emulator for the next step prediction implying that this downscaling operation can be considered to be a postprocessing approach that can be performed offline. We detail the various components of this approach in the following.

2.1 LUCIE

The coarse-grid dynamics that are used as inputs to the downscaling framework are provided by the LUCIE emulator (Guan et al., 2025). LUCIE (Lightweight Uncoupled Climate Emulator) is a data-driven atmospheric emulator designed to overcome the prohibitive computational costs of traditional numerical weather prediction and high-resolution ML models, which often require thousands of GPU hours. By leveraging an SFNO (Bonev et al., 2023) backbone and a specialized training strategy—including spectral regularization and a hard-constrained first-order integrator—LUCIE maintains long-term stability and physical consistency without the common unphysical drift in autoregressive models.

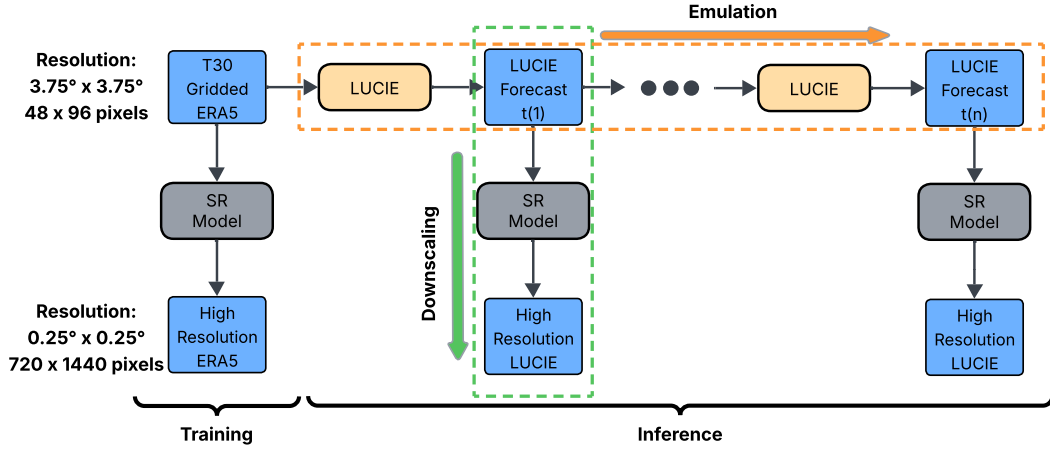


Figure 1. Schematic of the downscaling framework. **(Left) Training phase:** The downscaling model is trained on T30 gridded ERA5 data to learn the transformation from a coarse resolution to a high resolution. **(Right) Inference phase:** The trained downscaling model is applied to the coarse-resolution output from the LUCIE climate emulator to generate high-resolution climate projections.

The primary advantage of LUCIE lies in its computational efficiency; it can be trained in just 2.4 hours on a single A100 GPU and is capable of simulating 6,000 years of climate per day. However, the relatively coarse T30 Gaussian grid (3.75° resolution) is its main limitation. While this grid is sufficient for capturing large-scale dynamics and global climatology, it cannot resolve the fine-scale regional details necessary for localized studies.

This study proposes a downscaling framework as a critical bridge for this gap. By coupling LUCIE's stable, low-cost dynamical core with machine learning downscaling, we overcome the T30 resolution barrier and extend LUCIE's utility to regional-scale applications. This two-stage approach leverages the complementary strengths of both models: the computational efficiency of the lightweight emulator and the high-fidelity spatial reconstruction of the diffusion framework, enabling detailed analysis of local phenomena without the computational cost of end-to-end high-resolution training.

2.2 Data

For training our downscaling models, we use ECMWF Reanalysis v5 (ERA5) (Hersbach et al., 2020), a physically consistent, global atmospheric reanalysis available hourly on a 0.25° grid. ERA5 combines ECMWF's Integrated Forecasting System (IFS) with data assimilation of both conventional measurements and a wide range of satellite observations, providing a long, temporally consistent record from the mid-20th century to the present. For our SR experiments, the low-resolution inputs are ERA5 fields regridded to a T30 Gaussian grid ($\approx 3.75^\circ$) (Arcomano et al., 2022), while the high-resolution targets are the native 0.25° ERA5 fields. This pairing is chosen to enable zero-shot inference of the trained SR model with the LUCIE climate emulator, which itself operates on T30 Gaussian grid ERA5. To match the emulator's channel set, we include near-surface temperature at $\sigma = 0.95$ (≈ 963 hPa over ocean), zonal and meridional winds at $\sigma = 0.34$ (≈ 345 hPa over ocean), and surface precipitation. The training dataset is set to cover the year 2000 to year 2009 with samples at every 6 hour. The data is normalized by mean and standard deviation over the training period. For the deterministic mod-

els SFNO-SR and UNet-SR in this study, the input data is bicubic interpolated from 3.75° to 0.25° . All the models have 0.25° orography as the forcing variable (input only). The variables are listed in Table 1.

Table 1. The list of low-resolution input variables, high resolution target variables, the forcing variable, and their grid resolution. Model level 133 corresponds to ≈ 1000 hPa and model level 83 corresponds to ≈ 500 hPa

Category	Variables	Resolution
Input (Low-Res)	Temperature ($\sigma = 0.95$)	
	Zonal Wind ($u, \sigma = 0.34$)	T30 Gaussian
	Meridional Wind ($v, \sigma = 0.34$)	($\approx 3.75^\circ$)
	Surface Precipitation	
Target (High-Res)	Temperature (model level 133)	
	Zonal Wind (model level 83)	ERA5 Native
	Meridional Wind (model level 83)	(0.25°)
	Surface Precipitation	
Forcing (Static)	Orography	0.25°

2.3 SFNO-SR

Neural operators represent a machine learning framework that may be used to learn transformations between continuous function spaces. The Fourier Neural Operator (FNO) (Li et al., 2020) implements this by performing convolutions in the spectral domain, which allows for global spatial reasoning and inherent resolution-invariance. To account for the Earth’s geometry, the SFNO replaces standard Fourier Transforms with Spherical Harmonic Transforms (SHT). This ensures that the model respects the spherical coordinate system, avoiding the artifacts around boundaries that arise when processing global climate data on a flattened projection.

The SFNO-SR architecture leverages this framework to map four variables—temperature, zonal wind (u), meridional wind (v), and precipitation—from a 48×96 grid to a 720×1440 resolution ($15 \times$ upscaling). The process projects inputs into a 32-dimensional latent space, followed by four SFNO layers: an encoder, a spectral upscaling layer, and two high-resolution blocks (Bonev et al., 2023). These layers utilize SHTs and complex-valued kernels for spatial operations, interspersed with four 8-head self-attention blocks to capture long-range dependencies. A long skip connection connects the initial encoder directly to the final processing blocks. The model uses Gaussian Error Linear Unit (GELU) activations and instance normalization throughout. Training was conducted over 100 epochs using a Mean Absolute Error (L_1) loss function and the Adam optimizer with a learning rate of 0.001, following a cosine annealing schedule. This architecture was specifically chosen to maintain structural compatibility with the SFNO backbone utilized by the LUCIE climate emulator. While SFNO-SR may not currently deliver the most outstanding performance compared to generative alternatives as shown in the following chapters, utilizing a shared operator backbone creates a foundation for potentially embedding the SR model directly within the emulator in future iterations.

2.4 UNet-SR

The UNet is a specialized convolutional neural network architecture characterized by a symmetrical, U-shaped design that utilizes skip connections to bridge high-resolution features from an encoder path to a decoder path for spatial reconstruction. Building on

its success in image processing, the UNet architecture has been widely adapted for super-resolution within weather forecasting and atmospheric science (Sharma & Mitra, 2022; Zhang et al., 2024). We utilize the standard encoder-decoder UNet framework (Ronneberger et al., 2015) as our baseline UNet-SR model to perform spatial super-resolution on global climate data. The model operates on five input channels: the four primary weather variables (temperature, u wind, v wind, and precipitation) and a constant geopotential surface field. Prior to entering the network, the low-resolution T30 data is upsampled to the target 720×1440 resolution using bicubic interpolation, and precipitation values are normalized via a log-scaling transformation. The encoder path consists of four stages of downsampling, using 2×2 max-pooling and double 3×3 convolutions to increase the feature depth from 16 to a 256-channel bottleneck. The decoder path mirrors this structure, employing bilinear interpolation for upsampling and direct concatenation skip connections at each level to recover spatial details from the encoder. Each convolution is followed by Batch Normalization and ReLU activation. The model was trained for 100 epochs using Mean Absolute Error (L_1) loss and the Adam optimizer with a cosine annealing learning rate schedule.

2.5 Elucidating Diffusion Models (EDM)

We approach the generative modeling task using the diffusion framework, which models data generation as a reversal of a progressive noise corruption process (Sohl-Dickstein et al., 2015; Ho et al., 2020; Song et al., 2020). Specifically, we adopt the Elucidating Diffusion Model (EDM) formulation proposed by Karras et al. (2022), which provides a robust design space for score-based generative models. We perform conditional SR via input concatenation, and finally utilize an unconditional model with a posterior sampling strategy.

The forward process in the EDM framework describes the gradual corruption of a clean data sample $\mathbf{x}_0 \sim p_{\text{data}}(\mathbf{x})$ by additive Gaussian noise. Unlike standard SDE formulations, EDM parameterizes this corruption solely by the noise level σ , independent of a specific time schedule:

$$\mathbf{x}(\sigma) = \mathbf{x}_0 + \sigma \mathbf{n}, \quad \text{where } \mathbf{n} \sim \mathcal{N}(\mathbf{0}, \mathbf{I}). \quad (1)$$

The generative process involves solving a probability flow Ordinary Differential Equation (ODE) that traverses from a high-noise distribution (σ_{max}) back to the data distribution ($\sigma_{\text{min}} \approx 0$). The ODE is defined as:

$$d\mathbf{x} = \left[\frac{\mathbf{x}(\sigma) - \mathbf{x}_0}{\sigma} \right] d\sigma, \quad (2)$$

where the term in brackets represents the score function scaled by σ . To solve this numerically, a neural network F_θ is trained to estimate the clean data \mathbf{x}_0 from a noisy input. EDM introduces a preconditioning scheme to ensure the network inputs and outputs maintain unit variance during training. The effective denoiser D_θ is trained by minimizing the weighted L_2 error between the predicted and ground-truth data:

$$\mathcal{L}(\theta) = \mathbb{E}_{\mathbf{x}_0, \mathbf{n}, \sigma} [\lambda(\sigma) \|D_\theta(\mathbf{x}_0 + \sigma \mathbf{n}; \sigma) - \mathbf{x}_0\|_2^2], \quad (3)$$

where the weighting function is typically set to weight inputs at different noise levels differently. Refer Karras et al. (2022) for more details on these hyperparameters. Once the model is trained to predict the expected \mathbf{x}_0 at different noise levels, it is substituted in Equation 2 and integrated to obtain samples from the data distribution.

2.5.1 Conditional Downscaling

To adapt the EDM framework for SR, we modify the network to estimate the high-resolution field \mathbf{x}_0 conditioned on a low-resolution field \mathbf{y} . A straightforward and effective method for incorporating this condition is channel-wise concatenation.

Let $\mathcal{U}(\cdot)$ denote an upsampling operator (e.g., bicubic interpolation) that projects \mathbf{y} to the spatial resolution of \mathbf{x} . The neural network input is augmented to include this guidance information:

$$\mathbf{x}_{\text{in}} = \text{Concat}(\mathbf{x}(\sigma), \mathcal{U}(\mathbf{y})). \quad (4)$$

The denoiser becomes a conditional function $D_\theta(\mathbf{x}(\sigma), \mathbf{y}; \sigma)$. By providing the low-resolution context directly to the early layers of the model, the network learns to synthesize high-frequency details that are statistically consistent with the coarse-grained structures present in \mathbf{y} .

The conditional super-resolution framework utilizes a U-Net backbone optimized with EDM (Elucidating Diffusion Models) preconditioning. The architecture is designed for multi-variable atmospheric states, featuring 4 input/output channels—including temperature, winds, humidity, and precipitation—conditioned on 4 coarse-resolution T30 channels and orography from high resolution ERA5. To capture multi-scale atmospheric features without the computational overhead of self-attention, we employ a deep residual structure with 3 residual blocks per level and a progressive channel multiplier sequence of [1, 2, 4, 8, 16], starting from a base width of 32 channels. Group Normalization (32 groups) is applied throughout to maintain training stability across varying noise scales. Training was conducted using the EDM noise-weighted loss function ($P_{\text{mean}} = 0$, $P_{\text{std}} = 2$) to ensure high-fidelity reconstruction across all diffusion stages. The model was trained for 50 million snapshots on 16 NVIDIA A100 GPUs, using the AdamW optimizer with a 5 million snapshot linear warmup.

2.5.2 Posterior Sampling Downscaling

To generate samples consistent with partial or low-fidelity observations \mathbf{y} , we employ a posterior sampling strategy. By applying Bayes' rule, the score function of the posterior distribution $p(\mathbf{x}|\mathbf{y})$ decomposes into the learned prior score and a likelihood constraint:

$$\nabla_{\mathbf{x}} \log p(\mathbf{x}|\mathbf{y}) = \nabla_{\mathbf{x}} \log p(\mathbf{x}) + \nabla_{\mathbf{x}} \log p(\mathbf{y}|\mathbf{x}) \quad (5)$$

Evaluating the likelihood $p(\mathbf{y}|\mathbf{x}(\sigma))$ on noisy states is analytically intractable. Following methods like Diffusion Posterior Sampling (DPS) (Chung et al., 2022) and Score-based Data Assimilation (SDA) (Rozet & Louppe, 2023), we approximate this term using the denoised estimate of the data. Since the EDM denoiser directly predicts the clean data, i.e., $\hat{\mathbf{x}}_0 = D_\theta(\mathbf{x}(\sigma); \sigma)$, we can compute a likelihood score \mathbf{s}_l by backpropagating through the differentiable measurement operator \mathcal{M} :

$$\mathbf{s}_l(\mathbf{x}, \sigma; \mathbf{y}) \approx -\nabla_{\mathbf{x}} \frac{\|\mathbf{y} - \mathcal{M}(D_\theta(\mathbf{x}; \sigma))\|^2}{\Sigma_y + \sigma^2 \hat{\Gamma}} \quad (6)$$

The denominator represents the effective variance, combining the measurement noise covariance Σ_y with a time-dependent stability term $\sigma^2 \hat{\Gamma}$ derived from the SDA formulation (Rozet & Louppe, 2023), where $\hat{\Gamma}$ is a tunable constant approximating the Jacobian-prior interaction.

The posterior sampling model employs the same UNet with EDM preconditioning as the conditional SR model, maintaining 3 residual blocks per level and a channel multiplier sequence of [1, 2, 4, 8, 16]. A critical distinction lies in the conditioning: rather than using multi-level T30 variables directly, this model uses a single-channel bicubic upsampling of the low-resolution data. This configuration enables the model to serve as a learned prior for atmospheric states, where the reverse diffusion process is guided by the coarse input to satisfy the posterior distribution $p(x_0|y)$. The batch size is set to 48 per GPU. The model is trained on the native ERA5 dataset (using the 0.25° targets) for 50 million images (50,000 kimg) using the AdamW optimizer ($LR = 10^{-4}$). The loss function remains consistent with the EDM framework ($\sigma_{\text{data}} = 1.2$, $P_{\text{mean}} = 0$, $P_{\text{std}} = 2$).

This likelihood gradient guides the generation process by modifying the probability flow ODE. At each discretization step i , the standard EDM drift is adjusted to project the trajectory toward the measurement manifold:

$$\mathbf{d}_{\text{pos}} = \underbrace{\frac{\mathbf{x}_{\sigma_i} - D_{\theta}(\mathbf{x}_{\sigma_i}; \sigma_i)}{\sigma_i}}_{\text{Prior Drift}} - \lambda_g \cdot \sigma_i \cdot \mathbf{s}_l(\mathbf{x}_{\sigma_i}, \sigma_i; \mathbf{y}) \quad (7)$$

where λ_g is a guidance scale. The state is then updated using this posterior drift \mathbf{d}_{pos} , ensuring the final sample satisfies both the learned physics of the prior and the constraints of the observation \mathbf{y} . The full procedure is detailed in Algorithm 1 in (Chakraborty et al., 2025).

2.6 Computational Cost

All training was performed on NVIDIA A100 (80GB) GPUs using distributed data parallel training. Both the Conditional EDM and the posterior sampling framework required approximately 23 hours of training. For inference, the Conditional EDM generates 10 years of high-resolution data in 3.5 hours on a single GPU (≈ 68.5 years/GPU-day). In contrast, the posterior sampling method—which requires iterative gradient-based guidance—demands significantly higher resources, requiring 16 GPUs to generate a 10-year dataset in 4 hours (≈ 3.75 years/GPU-day). The deterministic SFNO-SR baseline is the most efficient, requiring 12.5 GPU-hours for training and 2.5 hours for 10-year inference (≈ 96.0 years/GPU-day) on a single GPU.

3 Results

This section evaluates the performance of the proposed super-resolution (SR) frameworks in downscaling global climate data, using the LUCIE model’s low-resolution outputs as a baseline. We assess the models across three critical aspects of atmospheric fidelity: climatological accuracy, where we examine long-term means and regional spatial fidelity; statistical consistency, using power spectra and probability density functions (PDFs) to verify the preservation of multiscale variability; and climate variability, through an EOF analysis of primary modes of atmospheric circulation. By comparing deterministic baselines (Bicubic, UNet-SR, SFNO-SR) against generative diffusion models (Conditional and Posterior Sampling EDM), we demonstrate the trade-offs between point-estimate precision and the reconstruction of physically realistic fine-scale structures.

3.1 Climatology

As a standard and informative indicator of climatological performance, we begin by evaluating the long-term climatological means of super-resolved near-surface temperature, zonal wind at 83 hPa, meridional wind at 83 hPa, and surface precipitation over 10 years of LUCIE inference from 2010–2019. Figure 2 presents these climatological fields for ERA5, bicubic interpolation, SFNO-SR, UNet-SR, conditional EDM, and posterior-sampling EDM. As expected for purely statistical downscaling, bicubic interpolation produces the major pattern in the climatological means but is missing fine details in the regional areas. The diffusion-based SR models generates high-resolution fields with accurate long-term average compared to UNet-SR and SFNO-SR, as reflected in the RMSE values summarized in Table 2: conditional EDM reduces the errors substantially across all variables, and posterior sampling achieves the lowest RMSE in temperature and zonal wind while maintaining competitive performance for meridional wind and precipitation. While deterministic baselines like UNet-SR achieve competitive RMSE, they exhibit a notable ‘variance deficit.’ As shown in Table 2, the temporal standard deviation for UNet-SR (4.9083 K) is significantly lower than that of the Diffusion-based models. This suggests that deterministic models produce oversmoothed fields and capture a smaller range

of climatological variability. However, despite the visual performance, EDM-based downscaling introduces ensemble variability due to its stochastic nature, resulting in higher RMSE compared with the deterministic LUCIE inference. For example, the posterior-sampling temperature field has an RMSE of 1.127 K compared with 0.727 K for native LUCIE outputs (Guan et al., 2025).

Beyond global averages, the fidelity of the EDM models is particularly evident when examining seasonal temperature extremes over the Contiguous United States (CONUS). In the June-July-August (JJA) Temperature Mean, the ERA5 ground truth reveals sharp thermal gradients driven by the complex topography of the Rocky Mountains and the Sierra Nevada. While the Bicubic, UNet-SR, and SFNO-SR approaches provide a generalized heat distribution, they suffer from spectral blurring and fail to resolve the cool-temperature “islands” associated with high-altitude peaks. In contrast, the EDM approaches recover these fine-scale structures with high precision, accurately capturing the thermal contrast in the Intermountain West and the Central Valley of California. Such localized accuracy is essential for downstream applications like assessing wildfire risk, where sub-grid temperature variations are decisive. During the December-January-February DJF period, the EDM models demonstrated superior skill in reconstructing cold air pooling in the Northern Plains and the sharp transition zones along the Appalachian range.

The zonal mean profiles in Figure 6 offer an easier way to see how these models differ on a global scale. While the spatial maps shown earlier focus on regional details, these latitudinal graphs provide a clear quantitative look at how well each model follows the ERA5 ground truth. Bicubic interpolation, SFNO-SR, and UNet-SR follow the general patterns of the atmosphere, but they are clearly less accurate than the Conditional EDM, especially when it comes to capturing sharp changes in tropical rainfall and wind patterns.

The most important takeaway from this comparison is the probabilistic nature of diffusion models. In the context of atmospheric science and nonlinear multiscale systems generally, SR forms an ill-posed inverse problem characterized by a one-to-many mapping. Specifically, a single low-resolution atmospheric state lacks sufficient constraints to uniquely determine a high-resolution realization, as multiple physically plausible fine-scale configurations can satisfy the same coarse-scale boundary conditions. Unlike deterministic methods that provide a single point estimate, generative models can sample from the prior distribution of possible high-resolution states, thereby capturing the inherent stochasticity and sub-grid scale variability of the climate system. It is worth noting that Posterior Sampling is also capable of creating these ensembles, but require significant computational resources. Generating just one ensemble of 10 year inference of LUCIE using posterior sampling takes 4 hours on 16 A100 GPUs. In contrast, the Conditional EDM is much faster, creating all 16 versions in only 3.5 hours with the same resources.

Table 2. Quadrature-weighted RMSE and Temporal Standard Deviation (STD) for various super-resolution models. Values are shown as RMSE (STD). The lowest RMSE value for each variable is in bold.

Variable	Bicubic	SFNO-SR	UNet-SR	Conditional	Posterior Sampling
Temperature [K]	2.581 (5.34)	2.497 (4.99)	2.427 (4.91)	1.357 (6.07)	1.237 (5.94)
U wind [m/s]	2.358 (11.61)	2.387 (11.79)	2.000 (11.54)	1.481 (12.97)	1.390 (11.83)
V wind [m/s]	0.933 (10.48)	0.780 (10.56)	0.815 (10.20)	0.770 (11.50)	0.798 (10.76)
Precipitation*	0.249 (0.8)	0.325 (0.7)	0.301 (0.6)	0.212 (1.1)	0.221 (1.3)

* Precipitation values for RMSE and STD are scaled by 10^3 for readability (10^{-3} m/6hr).

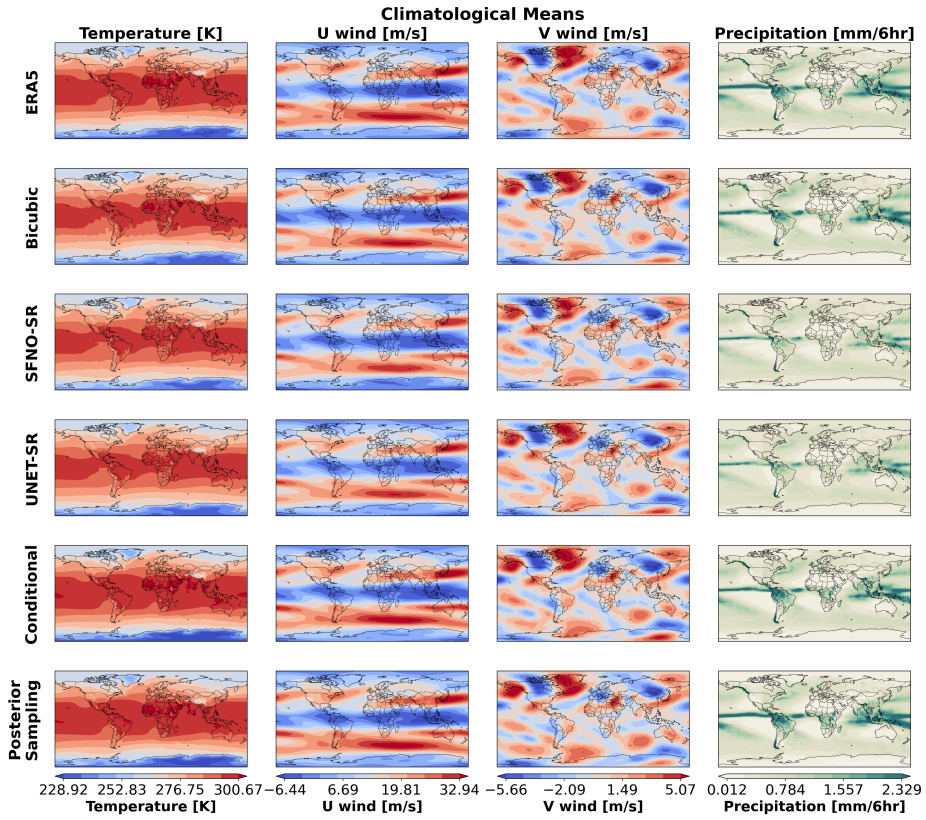


Figure 2. Super-resolved climatological snapshots averaged over the 2010–2018 period for 2m temperature, zonal wind, meridional wind, and precipitation. Coarse-grid dynamics for this period were generated by the LUCIE emulator and then downscaled with different super-resolution algorithms corresponding to the different rows. ERA5 reanalysis (our assumed ground truth) is provided in the first row from the top.

3.2 Power spectrum and extreme events

A significant strength of LUCIE is its ability to reproduce key statistical properties—including the zonal power spectrum, variance distribution, and return-period behavior—directly on the coarse T30 grid. Prior analyses have shown that LUCIE preserves the observed spectral slope across a wide range of scales and captures realistic distributional tails for temperature, winds, and precipitation. Therefore, a critical goal of the super-resolution in this work is not to correct deficiencies in LUCIE but to upscale its outputs while maintaining these desirable statistical properties on a finer grid.

To evaluate this, we examine the zonal power spectra (left column of Figure 7) and the corresponding PDFs on the right column. Bicubic interpolation, used as a baseline, exhibits severe damping of intermediate and high-wavenumber variance, reflecting the strong smoothing inherent to polynomial interpolation. In the low-wavenumber regime, SFNO-SR aligns reasonably well with the ERA5 reference. However, as the spatial scale decreases, its power spectrum begins to exhibit physically unrealistic wavy oscillations and periodic spikes in the high-wavenumber realm. These artifacts likely stem from the Fourier-based nature of the architecture, where aliasing or Gibbs-like phenomena can introduce artificial periodicities when attempting to reconstruct fine-scale turbulence. In contrast, both EDM-based methods retain much more of the original spectral structure. The conditional EDM restores a realistic spectral slope and captures a substantial por-

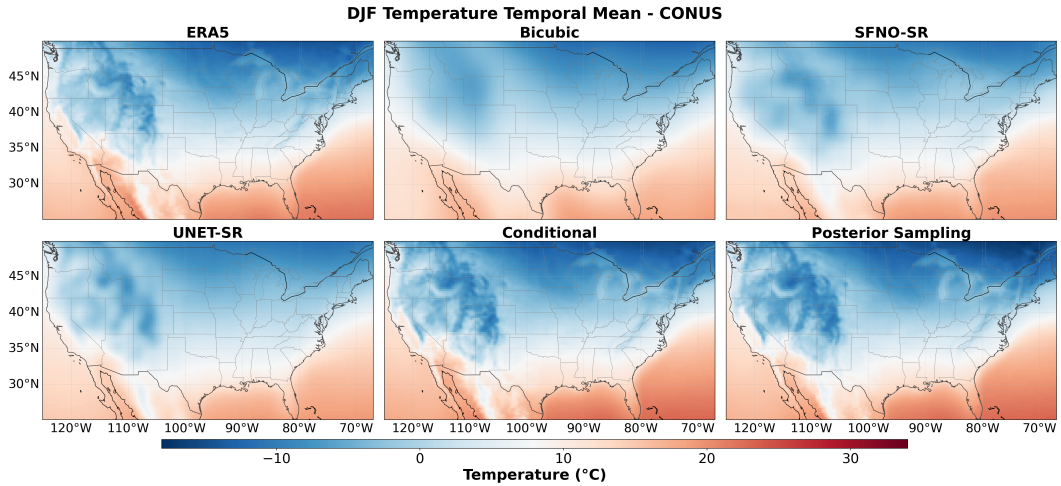


Figure 3. Climatological mean of ERA5, Bicubic interpolation, SFNO-SR, Conditional EDM, and EDM with Posterior Sampling in December, January, and February of temperature in CONUS area from 2010 to 2018.

tion of the missing high-wavenumber power, though it still underestimates the smallest scales relative to ERA5. The posterior-sampling EDM fits closely to the reference spectra, reproducing both the large-scale slope and the tail. This indicates that diffusion-based super-resolution can preserve LUCIE’s long-term variability during downscaling rather than artificially smoothing or amplifying it. The right column of Figure 7 demonstrates the models’ ability to capture the true distribution of atmospheric variables. The diffusion models capture the heavy tails and extremes much more accurately than bicubic interpolation. This is not surprising due to the ability of generative diffusion models to reconstruct fine details in the spatial field.

3.3 EOF of zonal wind

To evaluate how well each model captures dominant atmospheric patterns, an EOF analysis was performed on the zonal wind component. The first EOF mode (EOF1) represents the primary spatial pattern of variability, specifically the Northern Annular Mode (NAM) during the Northern Hemisphere winter (DJF) and the Southern Annular Mode (SAM) during the Southern Hemisphere winter (JJA).

In the Northern Hemisphere, ERA5 EOF1 shows a characteristic tri-polar structure, explaining 4.8% of the total variance. While Bicubic interpolation overestimates the northernmost anomaly at 5.2%, the deterministic SFNO-SR and UNet-SR models recover the spatial structure but overestimate variance at 6.4% and 6.1%, respectively. The generative models—Conditional (5.9%) and Posterior Sampling (6.2%)—provide the

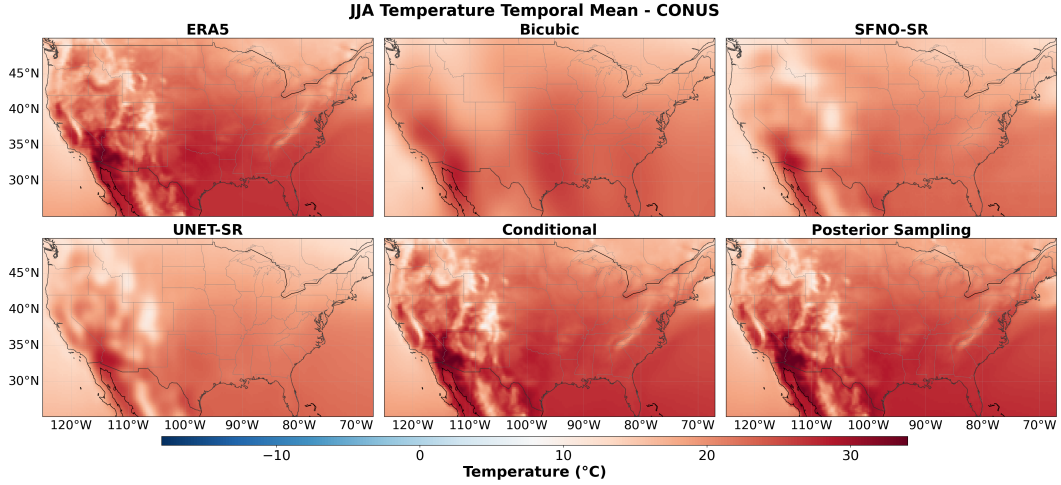


Figure 4. Climatological mean of ERA5, Bicubic interpolation, SFNO-SR, Conditional EDM, and EDM with Posterior Sampling in June, July, and August of temperature in CONUS area from 2010 to 2018.

most balanced representation of the reference centers of action. While the UNet-SR, Conditional, and Posterior Sampling models show consistent EOF patterns that do not perfectly match the ERA5 reference, they succeed in the framework’s core intention: faithfully recovering the dynamics of LUCIE as represented in the training distribution without introducing secondary distortions.

For the Southern Hemisphere, EOF1 illustrates the Southern Annular Mode, explaining 4.6% of the variance in the ERA5 data. All the models captures the general spatial pattern of ERA5. Both Bicubic and SFNO-SR models exhibit a spatial shift in the centers of action, with SFNO-SR notably overestimating variance at 6.1%. The UNet-SR (4.5%), Conditional (4.2%), and Posterior Sampling (4.3%) models accurately reconstruct the annular structure and the correct positioning of pressure centers. Similar to the Northern Hemisphere results, these models maintain a consistent internal EOF logic that reflects the LUCIE dynamics. Without distortions or corrections, the SR maintains the dynamics learned by LUCIE and reconstructs them in high resolution.

4 Discussion and Conclusions

In this study, we evaluate the viability of a two-stage modeling framework: using super-resolution (SR) models to upscale the coarse-grid outputs of a lightweight climate emulator. While our climate emulator, LUCIE, excels at capturing large-scale dynamics and global statistics, its utility for regional-scale analysis is inherently limited by its T30 Gaussian grid. We demonstrate that the introduction of an SR model effectively bridges

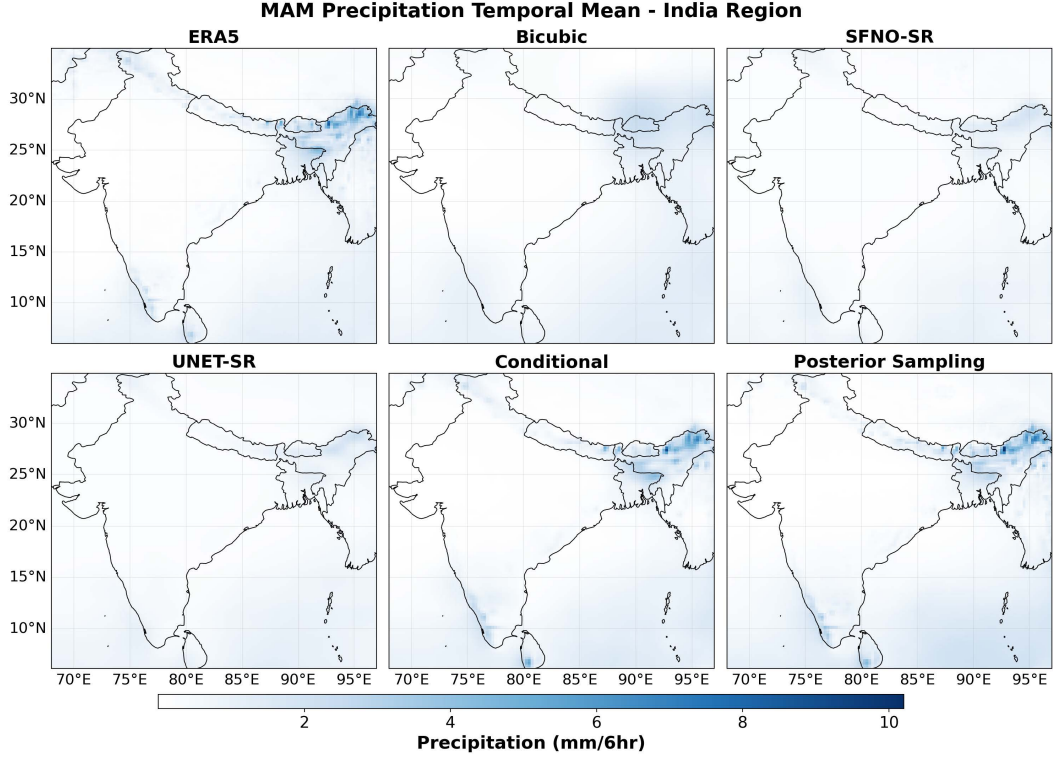


Figure 5. Temporal mean of precipitation over March, April, and May from 2010 to 2018 in India.

this gap, reconstructing the fine-scale spatial structures such as temperatures in the Rocky mountain area that are implied by the large-scale state but unresolved on the coarse grid.

A central finding of this work is that super-resolution serves as a faithful extension of the underlying emulator. Our evaluation shows that the SR process does not merely ‘smooth’ the data but actively restores the statistical properties of the system on a finer manifold. While deterministic baselines like bicubic interpolation and SFNO-SR capture the general atmospheric patterns, they often lack the precision required for regional studies. In contrast, the diffusion-based models (Conditional and Posterior-Sampling EDM) proved particularly adept at recovering localized features like precipitation over the Indian peninsula or thermal gradients in the Andes. By adding this spatial resolution, the combined LUCIE-SR framework makes it possible to conduct studies on monsoon-dependent agriculture or wildfire risk zones—applications that were previously beyond the reach of coarse-resolution emulators.

Furthermore, this work highlights the conceptual importance of the “one-to-many” mapping inherent in atmospheric downscaling. Because a single coarse-scale observation can physically correspond to multiple high-resolution configurations, a probabilistic approach is naturally suited for this task. The ability of diffusion models to generate an ensemble of realizations provides a measure of sub-grid scale uncertainty that deterministic models cannot offer. While SFNO-SR remains a competitive deterministic baseline, its tendency to introduce high-wavenumber spectral artifacts suggests that generative denoising processes may be more robust at capturing the turbulent “roughness” of the atmosphere.

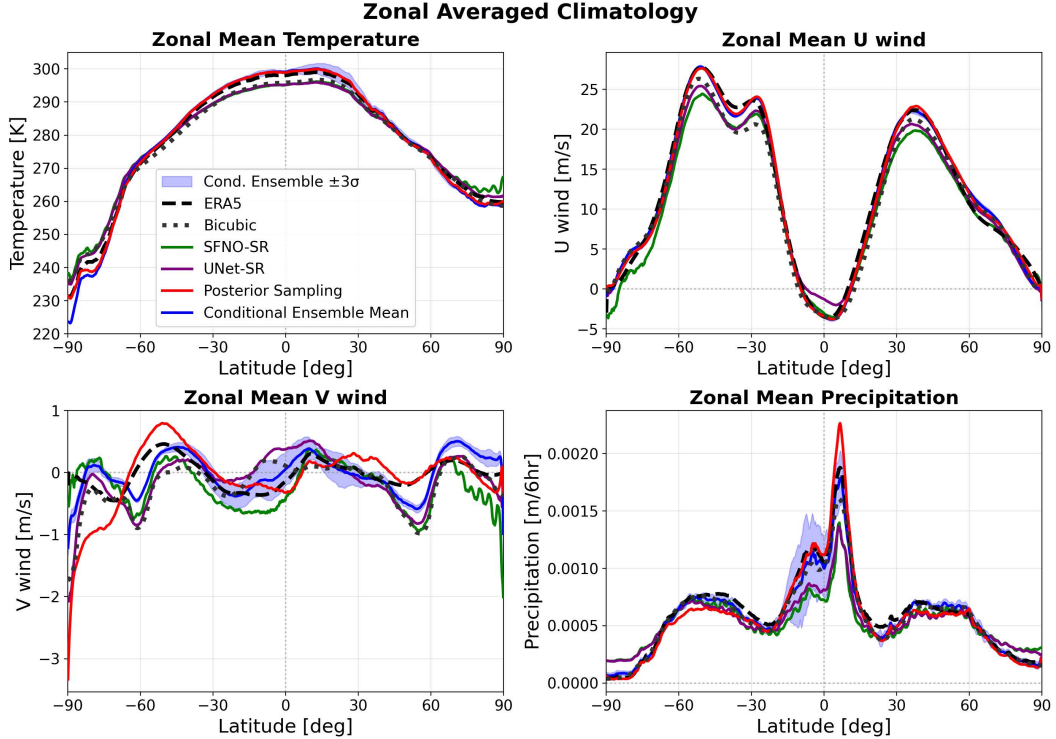


Figure 6. Latitude-weighted zonal climatology of temperature, U-wind, V-wind, and Precipitation from 2010 to 2018. The confidence interval of Conditional EDM is marked in blue shade.

The computational costs of these models vary significantly based on their architecture. The deterministic SFNO-SR is the fastest option, achieving a throughput of 96.0 years of samples per GPU-day. However, this speed results in visually smooth outputs that lack the fine-scale variability and sharp gradients found in high-resolution weather data. Diffusion-based models capture these details but require more time during inference. The Conditional EDM represents a practical solution; its training takes 23 hours, but its inference time is only 3.5 hours for a 10-year dataset—just one hour more than the deterministic baseline. This efficiency allows for the generation of the large ensembles that LUCIE is designed for. In contrast, posterior sampling is much more expensive to run, requiring 16 GPUs to produce 10 years of data in 4 hours, which results in a much lower throughput of 3.75 years per GPU-day. While posterior sampling is flexible because it does not require paired training, the conditional model is the more realistic choice for high-resolution emulation at scale. Another reason we included Posterior Sampling EDM in this study is the potential of adding observation data into the sampling process, without retraining a diffusion model, as shown in (Chakraborty et al., 2026). However, we also note that the conditional diffusion model removes the burden of constructing a likelihood function for the Bayesian posterior sampling process.

In summary, our results support a modular modeling strategy. By decoupling the simulation of large-scale climate dynamics from the reconstruction of spatial details, we can leverage the computational efficiency of models like LUCIE without sacrificing regional precision. This framework does not intend to “correct” the climate physics, but rather to complete the spatial picture. This two-stage approach offers a scalable, computationally efficient pathway for generating the high-resolution, ensemble-based data required for climate impact assessment and risk management.

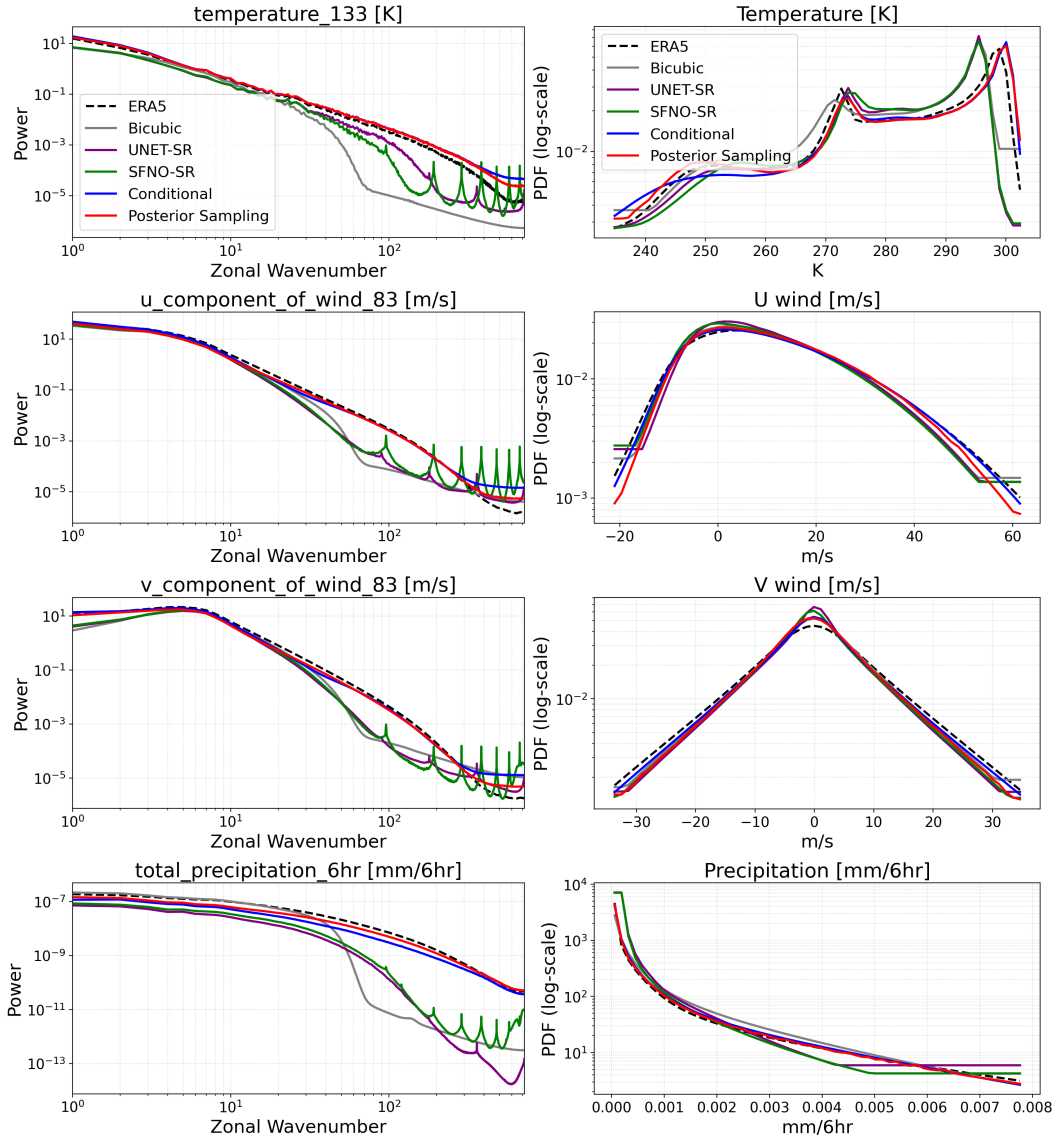


Figure 7. Comparison of mean spectral magnitudes across wavenumbers and PDFs for 2 m temperature, zonal wind, meridional wind, and precipitation. Curves correspond to Bicubic Interpolation, Conditional EDM, and Diffusion Posterior Sampling.

Open Research Section

The codes used for training and inference are permanently archived on Zenodo: (<https://zenodo.org/records/18627189>) Guan et al. (2026). The T30 Gaussian gridded ERA5 dataset required for training and the 10-year LUCIE emulation required for inference are included in the zenodo link. The high resolution ERA5 is available at: <https://doi.org/10.5065/XV5R-5344> (European Centre for Medium-Range Weather Forecasts, 2022).

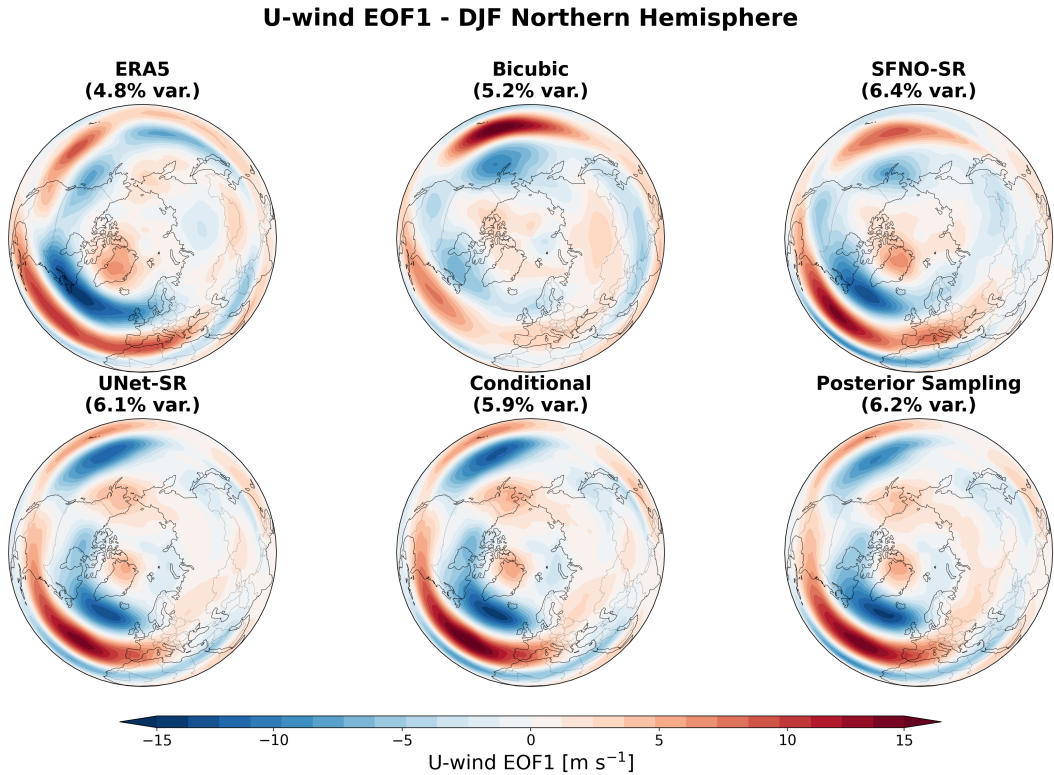


Figure 8. Comparison of the Northern Hemisphere Annular Mode (NAM) index. The EOF is computed over the full hemisphere using a latitude-based weighting of $\sqrt{\cos(\text{latitude})}$ to account for meridional area differences.

References

Arcomano, T., Szunyogh, I., Wikner, A., Pathak, J., Hunt, B. R., & Ott, E. (2022). A hybrid approach to atmospheric modeling that combines machine learning with a physics-based numerical model. *Journal of Advances in Modeling Earth Systems*, 14(3), e2021MS002712.

Baño-Medina, J., Manzanas, R., & Gutiérrez, J. M. (2020). Configuration and intercomparison of deep learning neural models for statistical downscaling. *Geoscientific Model Development*, 13(4), 2109–2124.

Bonev, B., Kurth, T., Hundt, C., Pathak, J., Baust, M., Kashinath, K., & Anandkumar, A. (2023). Spherical fourier neural operators: Learning stable dynamics on the sphere. In *International conference on machine learning* (pp. 2806–2823).

Chakraborty, D., Guan, H., Stock, J., Arcomano, T., Cervone, G., & Maulik, R. (2025). Multimodal atmospheric super-resolution with deep generative models. *arXiv preprint arXiv:2506.22780*.

Chakraborty, D., Guan, H., Stock, J., Arcomano, T., Cervone, G., & Maulik, R. (2026). Multimodal atmospheric super-resolution with deep generative models. *Machine Learning: Earth*, 2(1), 015001.

Chung, H., Kim, J., Mccann, M. T., Klasky, M. L., & Ye, J. C. (2022). Difusion posterior sampling for general noisy inverse problems. *arXiv preprint arXiv:2209.14687*.

European Centre for Medium-Range Weather Forecasts. (2022). *ERA5 Reanal-*

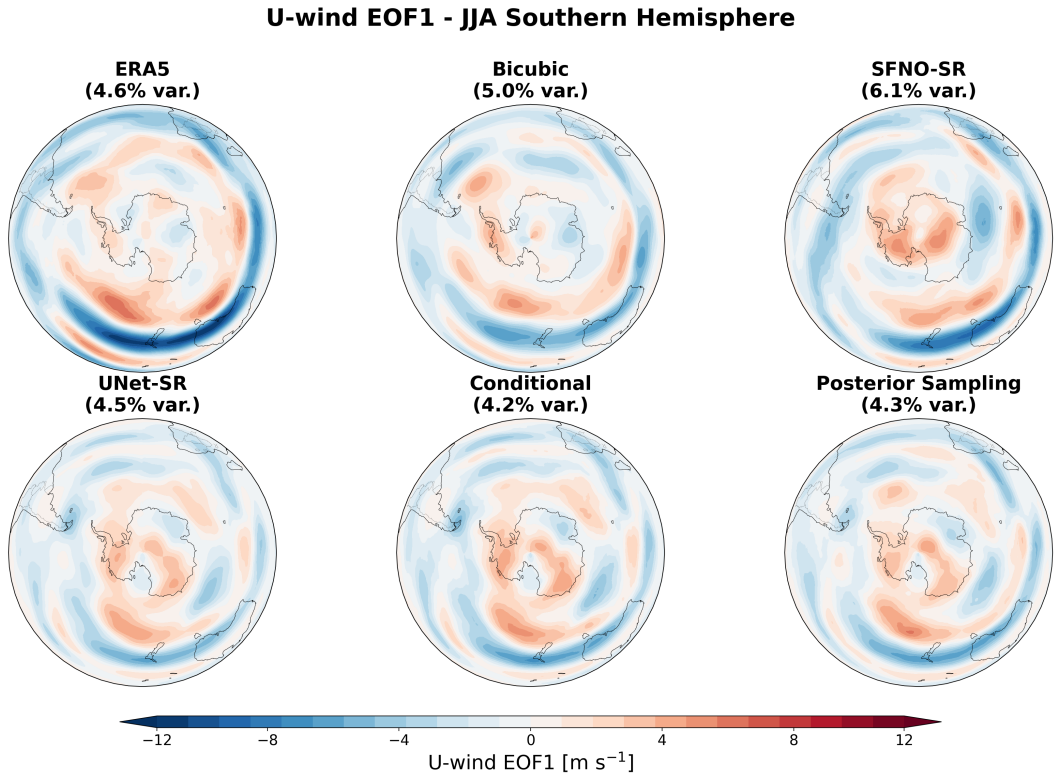


Figure 9. Comparison of the Northern Hemisphere Annular Mode (NAM) index. The EOF is computed over the full hemisphere using a latitude-based weighting of $\sqrt{\cos(\text{latitude})}$ to account for meridional area differences.

ysis Model Level Data. Boulder, CO: NSF National Center for Atmospheric Research. Retrieved from <https://doi.org/10.5065/XV5R-5344> doi: 10.5065/XV5R-5344

Giorgi, F. (2019). Thirty years of regional climate modeling: Where are we and where are we going after cordex? *Earth's Future*. doi: 10.1029/2019EF001341

Guan, H., Arcomano, T., Chattopadhyay, A., & Maulik, R. (2025). Lucie: A lightweight uncoupled climate emulator with long-term stability and physical consistency. *Journal of Advances in Modeling Earth Systems*, 17(11), e2025MS005152.

Guan, H., Darman, M., Chakraborty, D., Arcomano, T., Chattopadhyay, A., & Maulik, R. (2026, February). *High-resolution climate projections using diffusion-based downscaling of a lightweight climate emulator*. Zenodo. Retrieved from <https://doi.org/10.5281/zenodo.18627189> doi: 10.5281/zenodo.18627189

Harder, P., Schmidt, L., Pelletier, F., Ludwig, N., Chantry, M., Lessig, C., ... Rollnick, D. (2025). Rainshift: A benchmark for precipitation downscaling across geographies. *arXiv preprint*. Retrieved from <https://arxiv.org/abs/2507.04930>

Hersbach, H., Bell, B., Berrisford, P., Hirahara, S., Horányi, A., Muñoz-Sabater, J., ... others (2020). The era5 global reanalysis. *Quarterly journal of the royal meteorological society*, 146(730), 1999–2049.

Ho, J., Jain, A., & Abbeel, P. (2020). Denoising diffusion probabilistic models. *Advances in neural information processing systems*, 33, 6840–6851.

Jiang, P., Yang, Z., Wang, J., Huang, C., Xue, P., Chakraborty, T., ... Qian, Y.

(2023). Efficient super-resolution of near-surface climate modeling using the fourier neural operator. *Journal of Advances in Modeling Earth Systems*, 15(7), e2023MS003800.

Karras, T., Aittala, M., Aila, T., & Laine, S. (2022). Elucidating the design space of diffusion-based generative models. *Advances in neural information processing systems*, 35, 26565–26577.

Li, Z., Kovachki, N., Azizzadenesheli, K., Liu, B., Bhattacharya, K., Stuart, A., & Anandkumar, A. (2020). Fourier neural operator for parametric partial differential equations. *arXiv preprint arXiv:2010.08895*.

Lopez-Gomez, I., Wan, Z. Y., Zepeda-Núñez, L., Schneider, T., Anderson, J., & Sha, F. (2025). Dynamical-generative downscaling of climate model ensembles. *Proceedings of the National Academy of Sciences*, 122(17), e2420288122.

Maraun, D., & Widmann, M. (2018). *Statistical downscaling and bias correction for climate research*. Cambridge University Press.

Mardani, M., Brenowitz, N., Cohen, Y., Pathak, J., Chen, C.-Y., Liu, C.-C., ... others (2025). Residual corrective diffusion modeling for km-scale atmospheric downscaling. *Communications Earth & Environment*, 6(1), 124.

Nguyen, B. M., Tian, G., Vo, M.-T., Michel, A., Corpetti, T., & Granero-Belinchon, C. (2022). Convolutional neural network modelling for modis land surface temperature super-resolution. In *2022 30th european signal processing conference (eusipco)* (pp. 1806–1810).

Rampal, N., Hobeichi, S., Gibson, P. B., Baño-Medina, J., Abramowitz, G., Beucler, T., ... Gutiérrez, J. M. (2024). Enhancing regional climate downscaling through advances in machine learning. *Artificial Intelligence for the Earth Systems*, 3(2), 230066.

Reddy, P. J., Matear, R., Taylor, J., Thatcher, M., et al. (2025). Limitation of super-resolution machine learning approach to precipitation downscaling. *Scientific Reports*, 15. doi: 10.1038/s41598-025-05880-7

Ronneberger, O., Fischer, P., & Brox, T. (2015). U-net: Convolutional networks for biomedical image segmentation. In *International conference on medical image computing and computer-assisted intervention* (pp. 234–241).

Rozet, F., & Louppe, G. (2023). Score-based data assimilation. *Advances in Neural Information Processing Systems*, 36, 40521–40541.

Sachindra, D., Ahmed, K., Rashid, M. M., Shahid, S., & Perera, B. (2018). Statistical downscaling of precipitation using machine learning techniques. *Atmospheric research*, 212, 240–258.

Schwingshackl, C., Daloz, A. S., Iles, C., Aunan, K., & Sillmann, J. (2024). High-resolution projections of ambient heat for major european cities using different heat metrics. *Natural Hazards and Earth System Sciences*, 24, 331–354. doi: 10.5194/nhess-24-331-2024

Sharma, S. C. M., & Mitra, A. (2022). Resdeepd: A residual super-resolution network for deep downscaling of daily precipitation over india. *Environmental Data Science*, 1, e19.

Skamarock, W. C., Klemp, J. B., Dudhia, J., Gill, D. O., Barker, D. M., Wang, W., & Powers, J. G. (2019). A description of the advanced research wrf model version 4. *NCAR Technical Note*.

Sohl-Dickstein, J., Weiss, E., Maheswaranathan, N., & Ganguli, S. (2015). Deep unsupervised learning using nonequilibrium thermodynamics. In *International conference on machine learning* (pp. 2256–2265).

Song, Y., Sohl-Dickstein, J., Kingma, D. P., Kumar, A., Ermon, S., & Poole, B. (2020). Score-based generative modeling through stochastic differential equations. *arXiv preprint arXiv:2011.13456*.

Stengel, K., Glaws, A., Hettinger, D., & King, R. N. (2020). Adversarial super-resolution of climatological wind and solar data. *Proceedings of the National*

Academy of Sciences, 117(29), 16805–16815.

Tu, S., Fei, B., Yang, W., Ling, F., Chen, H., Liu, Z., et al. (2025). Satellite observations guided diffusion model for accurate meteorological states at arbitrary resolution. *arXiv preprint*. Retrieved from <https://arxiv.org/abs/2502.07814>

Tu, S., Xu, J., Yang, W., Bai, L., & Fei, B. (2025). Mods: Multi-source observations conditional diffusion model for meteorological state downscaling. *arXiv preprint*. Retrieved from <https://arxiv.org/abs/2506.14798>

Vandal, T., Kodra, E., Ganguly, S., Michaelis, A., Nemani, R., & Ganguly, A. R. (2017). Deepsd: Generating high resolution climate change projections through single image super-resolution. In *Proceedings of the 23rd ACM SIGKDD international conference on knowledge discovery and data mining* (pp. 1663–1672).

Wang, X., Sun, L., Chehri, A., & Song, Y. (2023). A review of gan-based super-resolution reconstruction for optical remote sensing images. *Remote Sensing*, 15(20), 5062.

Wei, M., & Zhang, X. (2023). Super-resolution neural operator. In *Proceedings of the IEEE/CVF conference on computer vision and pattern recognition* (pp. 18247–18256).

Zhang, L., Yang, A., Amor, R. A., Zhang, B., & Rao, D. (2024). Super resolution on global weather forecasts. *arXiv preprint arXiv:2409.11502*.

Zhu, X., Zhang, L., Zhang, L., Liu, X., Shen, Y., & Zhao, S. (2020). Gan-based image super-resolution with a novel quality loss. *Mathematical Problems in Engineering*, 2020(1), 5217429.